

CrystEngComm

Accepted Manuscript



This is an *Accepted Manuscript*, which has been through the Royal Society of Chemistry peer review process and has been accepted for publication.

Accepted Manuscripts are published online shortly after acceptance, before technical editing, formatting and proof reading. Using this free service, authors can make their results available to the community, in citable form, before we publish the edited article. We will replace this *Accepted Manuscript* with the edited and formatted *Advance Article* as soon as it is available.

You can find more information about *Accepted Manuscripts* in the [Information for Authors](#).

Please note that technical editing may introduce minor changes to the text and/or graphics, which may alter content. The journal's standard [Terms & Conditions](#) and the [Ethical guidelines](#) still apply. In no event shall the Royal Society of Chemistry be held responsible for any errors or omissions in this *Accepted Manuscript* or any consequences arising from the use of any information it contains.



Novel in-situ self-separation of 2-in. free-standing *m*-plane GaN wafer from *m*-plane sapphire substrate by HCl chemical reaction etching in hydride vapor-phase epitaxy

Received 00th January 20xx,
Accepted 00th January 20xx

DOI: 10.1039/x0xx00000x

www.rsc.org/

Seohwi Woo,^a Sangil Lee,^a Uiho Choi,^a Hyunjae Lee,^b Minho Kim,^b Jaiyong Han^b and Okhyun Nam^{a,*}

A 2-in.-diameter free-standing *m*-plane GaN wafer was fabricated through in-situ self-separation using HCl chemical reaction etching (HCRE) in hydride vapour-phase epitaxy (HVPE). A 2- μm -thick *m*-plane GaN layer was directly grown on *m*-plane sapphire, followed by HCRE to form multiple voids at the interface between the *m*-plane sapphire and *m*-plane GaN. Void formation was attributed to preferential etching at high-defect regions (HDRs) such as stacking faults (SFs) and threading dislocations (TDs) in the *m*-plane GaN layer. After regrowth of an approximately 200- μm -thick *m*-plane GaN layer, self-separation was achieved during the cooling process. The free-standing *m*-plane GaN wafer was almost crack-free as a result of strain relief by the in-situ self-separation process, which was confirmed by room-temperature Raman and photoluminescence measurements. It is supposed that the novel HCRE process can be applied to fabricate high-quality free-standing non-polar GaN wafers in the future.

Introduction

GaN, one of the Group III-nitride materials, has been gaining considerable attention as a material suitable for use in high-performance electronic and optoelectronic devices because of its excellent physical properties, such as its wide band gap, high thermal conductivity, and high breakdown voltage.¹ These devices, which are grown on the conventional polar (0001) plane, typically exhibit spontaneous and piezoelectric polarization effects that render them undesirable. The polarization effect causes band bending and reduces the radiative recombination efficiency in quantum wells (QWs), which in turn reduces the luminous efficiency of the devices due to the quantum-confined stark effect.² To eliminate this polarization effect, these devices must be grown on {11-22} semi-polar planes or on non-polar {11-20} α -plane GaN or {10-10} *m*-plane GaN (*m*-GaN). *m*-GaN, in particular, is more stable and has a wider acceptable range of growth conditions than {11-20} α -plane GaN.³ It also has a lower threading dislocation density than α -plane GaN,³ and it more readily accepts Mg, which enables *p*-type doping levels to be increased.⁴

Consequently, the use of *m*-GaN in an optical device with a multi-QW structure will improve the device performance. Because of these advantages, many research groups have

reported heteroepitaxial *m*-GaN films grown on LiAlO₂,⁵ *m*-plane SiC,⁶ patterned (112) Si,⁷ *m*-plane ZnO,⁸ and *m*-plane sapphire (*m*-sapphire).⁹⁻¹¹ Among these, *m*-sapphire is the best substrate choice for the growth of *m*-GaN because it is cost effective and larger substrate diameters are more readily available than those for LiAlO₂, SiC, or ZnO substrates.

Moreover, *m*-sapphire is more chemically and thermally stable than either LiAlO₂ or ZnO. In spite of these advantages, *m*-GaN grown directly on *m*-sapphire has a number of critical problems. In particular, high defect densities and an anisotropic crystal structure may occur because an antiphase domain boundary is formed by ambidirectional nucleation of *m*-GaN.¹² In addition, growing thick *m*-GaN leads to breakage during cooling and after unloading because of anisotropic stresses related to thermal expansion (*c*-axis: 34.2% compressive, α -axis: 3.3% tensile) and lattice mismatch (*c*-axis: 1.8% tensile, α -axis: 8.9% compressive) between *m*-GaN and *m*-sapphire.

To avoid these problems, commercially available *m*-GaN substrates with a low defect density and high isotropic crystal quality are produced from small transverse slices of *c*-oriented bulk crystals grown by HVPE.^{13,14} However, the small substrate size (a few square millimetres), high substrate cost, and complicated process have been proven to be serious drawbacks for industrial applications. For these reasons, further studies are required to prepare large-size (over 2-in.) crack-free, free-standing (FS) *m*-GaN wafers successfully.

In this paper, we successfully fabricated for the first time a crack- and stress-free 2-in.-diameter FS *m*-GaN wafer that was directly self-separated in-situ from an *m*-sapphire substrate by

^a Convergence Center for Advanced Nano Semiconductor (CANS), Department of Nano-Optical Engineering, Korea Polytechnic University (KPU), Siheun-si, Gyeonggi-do 429-793, Republic of Korea.

^b Lumistal Co., Ltd., Business Incubation Center, KPU, Korea, Republic of Korea.

* E-mail: ghnam@kpu.ac.kr

HVPE. The previous reports used the mechanical lapping of sapphire,¹⁵ laser lift-off,¹⁶ void-assisted separation by TiN,¹⁷ epitaxial lateral overgrown GaN,¹⁸ associated nanorod separation,¹⁹ ex-situ wet chemical etching,²⁰ and high-temperature annealing of a porous template.²¹ Furthermore, these methods were applied only to *c*-plane polar GaN (*c*-GaN).

Based on self-separation method for fabricating the 2-inch FS *m*-GaN wafer was demonstrated by Sasaki et al., in 2009. However, this study had additional ex-situ method process for deposited Al₄C₃ and AlN buffer layer on *m*-sapphire substrate by MOCVD. After ex-situ process, bulk thick *m*-GaN layer was regrown by HVPE.²²

Our self-separation method does not include any ex-situ processes to separate the GaN layer from a substrate after growth (only a one-step process in an HVPE reactor). Moreover, it is expected that the proposed method will provide a way to fabricate large-sized, FS *m*-GaN on *m*-sapphire substrates in the near future.

Experiments

The *m*-GaN template was grown on *m*-sapphire substrate with a 2° miscut with respect to the *a*-axis using an atmospheric HVPE system with a vertical reactor heated by a two-zone furnace. The substrate was heated up to 1050 °C during growth and etching. The source gases were NH_{3(g)} and GaCl_(g), with the latter being formed by the reaction between Ga_(l) and HCl_(g). Nitrogen (N₂) was used as the carrier gas.

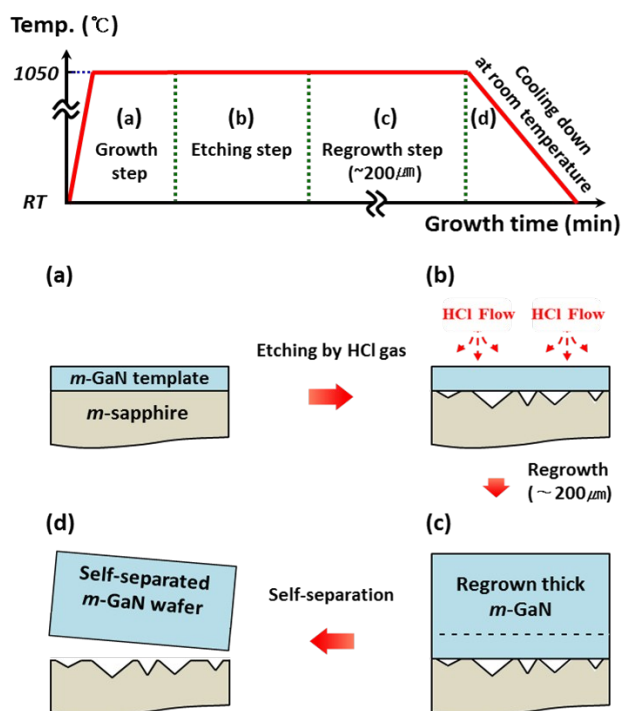


Fig. 1 Schematic diagrams of fabrication steps of a self-separated FS *m*-GaN wafer using in-situ HCRE. (a) *m*-GaN template growth (approximately 2-μm-thick), (b) penetration of HCl gas into interface and start of *m*-sapphire etching, (c) thick *m*-GaN regrowth (approximately 200-μm-thick), and (d) the self-separation of thick *m*-GaN layer from *m*-sapphire substrate during cooling to RT.

involved in the fabrication of a self-separated FS *m*-GaN wafer grown on *m*-sapphire are shown in Fig. 1.

First, a 2-μm-thick *m*-GaN template was grown directly on *m*-sapphire by HVPE at 1050 °C for 7 min, as shown in Fig. 1(a); the details of the HVPE process are described elsewhere.²³ Next, the *m*-GaN template was etched in the HVPE by flowing HCl gas prior to thick *m*-GaN regrowth by HVPE, as shown in Fig. 1(b). Then, a 200-μm-thick *m*-GaN layer was directly regrown in-situ on an etched *m*-GaN template at 1050 °C for 180 min, as shown in Fig. 1(c). Finally, during the cooling process, the 200-μm-thick *m*-GaN layer was self-separated from the underlying host *m*-sapphire substrate as a result of the release of thermal strain, as shown in Fig. 1(d). For comparison, a conventional 200-μm-thick *m*-GaN template was also grown on an *m*-sapphire substrate by HVPE.

The surface and cross-sectional morphology of the *m*-GaN layers were observed by optical microscopy (OM) and scanning electron microscopy (SEM), and the crystal quality was determined by omega rocking curves with High-resolution X-ray diffraction (HRXRD). Structural characteristics of the etched *m*-GaN were investigated using 200kV transmission electron microscope (TEM) (JEM-2100F+Cs corrector - JEOL/CEOS). The cross-sectional TEM sample was prepared by a focused ion beam (FIB) (Quanta 3D FEG (FEI)) process. Raman spectroscopy (Horiba Jobin-Yvon LabRam Aramis spectrometer) at room temperature (RT) using the 632.8 nm line of a He-Ne laser as the excitation source was employed to identify the stress in the as-grown thick *m*-GaN template and the self-separated FS GaN wafer. The Raman-scattered light signal was collected from a backscattering geometry using an x50 microscope objective lens. The Raman excitation beam spot size was approximately 1 μm in diameter (Raman grating vs. resolution 2400/gr, 0.3 cm⁻¹). The measured *E*₂ high value (567.6 cm⁻¹) confirmed almost zero strain in the substrates. The optical properties were determined by RT photoluminescence (PL) measurements with a 325 nm He-Cd laser as the excitation source. The PL measurements had a grating of 1200 grooves/mm (Resolution: point-to-point = ~ 0.003eV).

Results and discussion

Figure 2(a) shows the Nomarski bright-field mode (NBM) OM surface image of the as-grown *m*-GaN template. The *m*-GaN template did not have any cracks or pits. Figures 2(b) and (c) show the NBM-OM surface image of the *m*-GaN template with approximately 40% and 80% etching, respectively. It seems that the *m*-GaN template was etched at the interface between *m*-sapphire and *m*-GaN (red arrows and bright yellow dot regions) by HCl gas.

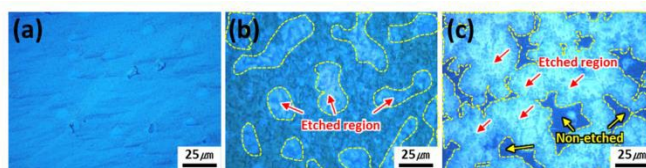


Fig. 2 NBM-OM surface images of (a) the as-grown 2-μm-thick *m*-GaN, *m*-GaN template etched by (b) 40% and (c) 80% in HCl gas, respectively.

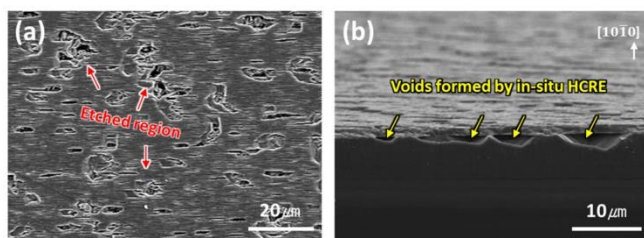


Fig. 3 SEM images of plan-view (a) and bird-eye view (b) of a 2- μm -thick *m*-GaN template layer on *m*-sapphire substrate etched in HCl gas. The red arrows indicate etched region of *m*-GaN surface. The yellow arrows indicate voids formed at the interface between *m*-sapphire and the *m*-GaN template layer.

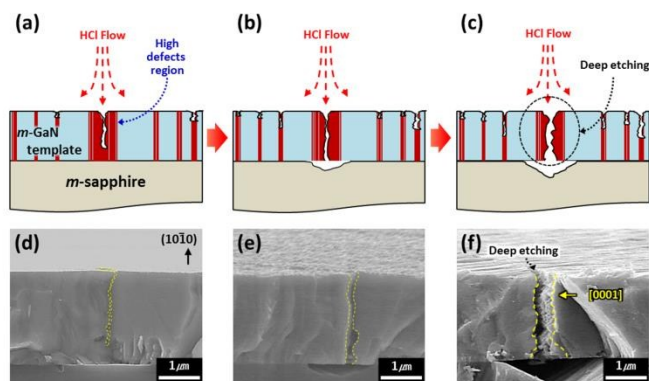


Fig. 4 Schematic diagrams (a)–(c) and cross-section SEM images (d)–(f) showing void formation mechanism at the interface between *m*-sapphire and *m*-GaN by in-situ HCRE. Selective etching at HDRs such as SFs and dislocations (a), (d). HCl penetration into interface and start to etching of the *m*-sapphire surface (b), (e). Deep etching of *m*-sapphire surface (c), (f).

Figure 3 shows the SEM images of plan-view (a) and bird-eye view (b) of the etched 2- μm -thick *m*-GaN template layer. Through HCRE process, the smooth and pit-free surface of *m*-GaN was etched by HCl gas, and changed into rougher surface with many etched pits. Also, it was confirmed that many voids were formed at the interface between *m*-sapphire and *m*-GaN by HCRE. The etched regions observed in OM surface images of Fig. 2 were actually the voids between *m*-sapphire and *m*-GaN. Interestingly, the low defect regions of the *m*-GaN layer were not nearly etched, whereas HDRs were preferentially etched.

In addition, the sizes of the voids on the *m*-sapphire were approximately several micrometres, as shown in Fig. 3.

Next, the formation of voids at the interface between *m*-sapphire and *m*-GaN was investigated. Figure 4 shows cross-sectional schematic images of the void-formation mechanism as a result of etching by HCl gas (Figs. 4(a–c)), and the corresponding SEM images (Figs. 4(d–f)). The cross-sectional schematic images show that HCl permeates preferentially into the HDR with increasing etching time (1, 9, and 25 min). This observation implies that the HDR was likely to be removed during the etching process by HCl gas.

Generally, cone-shaped nanoparticles or nanorods are found in etched *c*-GaN.^{24,25} However, in the case of *m*-GaN, those shapes were not observed, and the surface of the *m*-plane remained flat with almost no etching because the easily

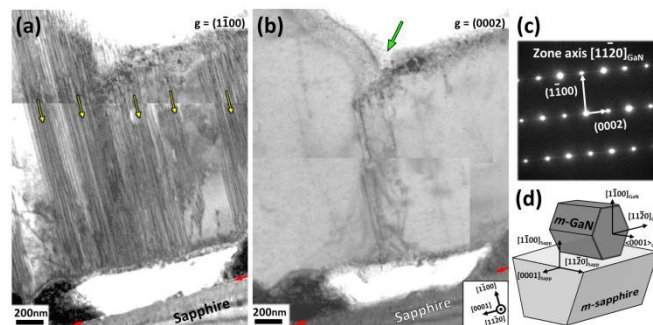


Fig. 5 Cross-sectional TEM bright-field images of etched *m*-GaN template layer obtained for different g vectors. (a) $g = 1-100$ [SFs are visible], (b) $g = 0002$ [TDs are visible], (c) the corresponding diffraction SAED patterns and (d) schematic showing epitaxial relationship of *m*-GaN on *m*-sapphire, respectively. The yellow arrows in Fig. (a) indicate the high density of SFs formed in *c*-planes, and the green arrow in Fig. (b) indicates TDs. (The image was taken in a two beam condition with $g = 1-100$ and $g = 0002$ near the $[11-20]_{\text{GaN}}$ zone axis)

etched dislocations were formed parallel to the growth plane in the crystal structure of *m*-GaN. However, in the process of *m*-GaN growth, vertical SFs also occur and are affected by the etching.²⁵ In general, the surface stripes in nonpolar GaN originate from different adatom growth rates in the two orthogonal in-plane directions.^{27,28} It was reported that the surface morphology of nonpolar GaN evolution during the two-step growth can be accounted for by the kinetic Wulff plots, which control the advances of crystallographic planes with complex geometries.^{27,28} Moreover, these surface stripes have been attributed to intersections of basal-plane SFs with the growth surface.²⁶⁻²⁸

The thickness of *m*-GaN remained almost unchanged, although the etching proceeded mainly at HDRs such as SFs and TDs, etc. It was confirmed that HCl permeated deeply and widely into the GaN layer, which formed the voids at the interface between *m*-sapphire and *m*-GaN by HCl, as shown in Figs. 3(d–f). According to previous research, HCl etching on *c*-GaN is activated in different types of surface energy relevant to each GaN plane (*c*-, *a*-, *r*-, and *m*-planes) as well as by defects.^{29,30} Previous research on the basis of a kinetic Wulff plot reported that the surface energy of the $[1-100]$ *m*-plane was the most stable (not etched by HCl),²⁵ which agrees with the results of this study. The *m*-plane, with no defects and stable energy, was not etched, although the HDRs were preferentially etched. We speculated that the areas etched by HCl were in an unstable energy state because of SFs and TDs caused by the ambidirectional growth mode of *m*-GaN.

We performed the TEM analyses to confirm the etching mechanism. Figure 5 shows the cross-sectional TEM images near the surface of the etched *m*-GaN layer after HCRE, which were obtained for the different g vectors of (a) $g = 1-100$ and (b) $g = 0002$ near the $[11-20]_{\text{GaN}}$ zone axis. The SFs and TDs are visible at (a) $g = 1-100$ and (b) $g = 0002$, respectively.¹⁰

Figure 5(c) shows the corresponding selected area electron diffraction (SAED) patterns taken from *m*-GaN. The incident beam was parallel to $[11-20]_{\text{GaN}}$ zone axes. Figure 5(d) shows epitaxial relationship between *m*-GaN and *m*-sapphire of $[1-100]_{\text{GaN}} // [1-100]_{\text{Sapphire}}$ and $[11-20]_{\text{GaN}} // [0002]_{\text{Sapphire}}$. Figure 5(d)

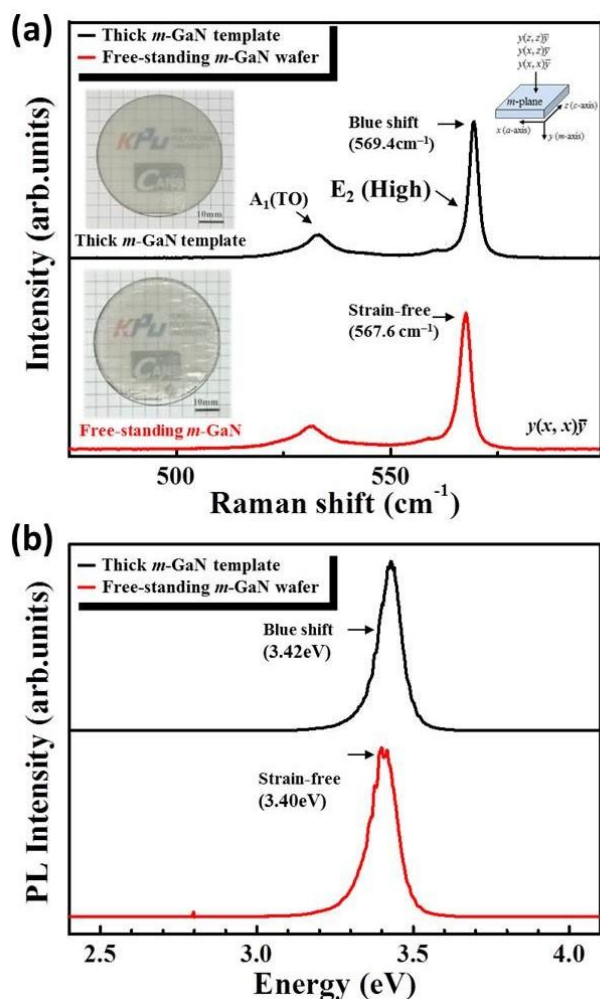


Fig. 6 (a) Raman scattering and (b) RT-PL results of as-grown thick *m*-GaN template and self-separated FS *m*-GaN wafer. The insets of Figure (a) show the as-grown thick *m*-GaN template and self-separated FS *m*-GaN wafer, respectively.

and HR-TEM analysis (Fig. S1(a)) provide direct evidence for the structural relationship of *m*-GaN and *m*-sapphire substrate.

The TEM results show that the HDRs such as the SFs and TDs are closely connected with the void formation mechanism by the HCRE.

In the case of *m*-GaN etched for 25 min, most of the semipolar {1-101} facets were exposed whilst the (0001) plane with relatively unstable energy was etched, as shown in Fig. 3(f).²⁵

The voids were formed at the interface between *m*-sapphire and *m*-GaN by etching of the *m*-plane of *m*-sapphire because the *m*-plane of *m*-sapphire was relatively unstable at high temperatures. The *m*-plane of sapphire (α -Al₂O₃) has been reported to be a thermodynamically unstable facet.³¹ Thus, the unstable *m*-plane of sapphire at high temperatures was etched by HCl to form micro-sized voids shaped like inverted triangles composed of *r*-plane and *s*-plane facets.³² The chemical reaction between sapphire and HCl could be described as follows:

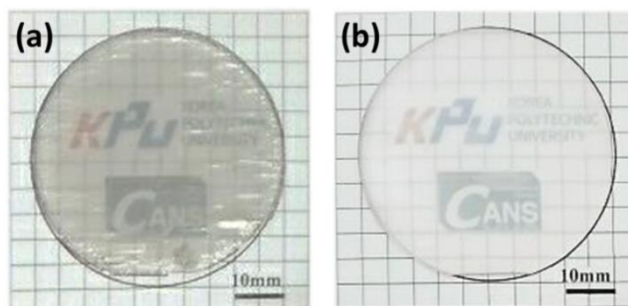


Fig. 7 Digital photograph-images of self-separated 2inch FS *m*-GaN wafer (a) and separated *m*-sapphire substrate (b).

In addition, in order to identify the difference in stresses between these two samples, we performed micro-Raman scattering analysis. The *E*₂ (high) phonon modes of the GaN substrates obtained from the thick *m*-GaN template and FS *m*-GaN wafer were located at 569.4 and 567.6 cm⁻¹, respectively, as shown in Fig. 6(a). The *E*₂ (high) peak of the FS *m*-GaN wafer was very close to that of the stress-free GaN substrate, which was reported to be 568 cm⁻¹.³³ Therefore, the residual stress of the FS *m*-GaN wafer was negligible. The residual stress can be calculated by the following equation:³⁴

$$\Delta\omega_\gamma = \omega_\gamma - \omega_0 = K_\gamma \cdot \sigma \quad (2)$$

where ω_γ and ω_0 represent the Raman peaks of GaN from the thick *m*-GaN template and the FS *m*-GaN wafer, respectively.

The relaxation of residual strain can be measured using the following equation:

$$\sigma = \frac{\Delta\omega}{4.2} (\text{cm}^{-1} \text{ GPa}^{-1}) \quad (3)$$

where σ is the biaxial stress and $\Delta\omega$ is the *E*₂ phonon peak shift.

A blue shift of 1.8 cm⁻¹ corresponds to a relaxation of compressive stress. The estimated value of the stress was found to be approximately 0.43 GPa by adopting the theoretical *K*_γ value of 4.2 cm⁻¹/GPa reported by C. Kisielowski et al.³⁵ The large difference in stress between these two samples was mainly due to relaxation of thermal stress, which inherently accumulated during the cooling process. The results suggest that the GaN crystal regrown on the self-separated FS *m*-GaN wafer had reduced biaxial stress, which could be advantageous for the growth of high-quality GaN.

We also examined the optical properties of the two samples. A 325-nm He–Cd laser was used to perform RT-PL measurement, and the laser output power was set at a constant 10 mW.

Figure 6(b) shows the PL spectra of near band-edge emission (NBE) obtained from the as-grown thick *m*-GaN template and self-separated FS *m*-GaN wafer. The NBE peaks were located at 3.42 eV and 3.40 eV, respectively. For the as-grown thick *m*-GaN template, a blue shift of the band-edge emission peak of approximately 0.02 eV was observed. It is known that the band-gap energy is affected by the residual stress in semiconductor thin films. Therefore, the red shift of the band-edge emission peak in the self-separated FS *m*-GaN wafer can be attributed to the relief of the compressive stress in the GaN crystal.

In addition to the Raman scattering measurement, this is clear evidence that our proposed scheme can provide a GaN substrate that is free of residual strain. HRXRD omega rocking curves were also employed to investigate the crystalline quality of the as-grown thick *m*-GaN template and self-separated FS *m*-GaN wafer (as shown Fig. S3). Although the results are not shown here, the full width at half maximum (FWHM) of the (10-10) peaks of the as-grown thick *m*-GaN template were 5750 and 1370 arcsec, respectively, for scan directions of [0001] and [11-20] GaN. In contrast, for the self-separated FS *m*-GaN wafer, the FWHM values were substantially reduced to 2240 and 820 arcsec, respectively, indicating improvement in the crystal quality. The crystal quality of the self-separated FS *m*-GaN must be improved further for practical use, and an additional study is underway to reduce the defect density of the self-separated FS *m*-GaN wafer.

Figure 7 shows digital photograph-images of the self-separated FS *m*-GaN wafer (a) and the separated *m*-sapphire substrate (b). A FS *m*-GaN wafer was successfully obtained, as shown in Fig. 7. However, the self-separated FS *m*-GaN wafer had some ripples on the surface, which was probably induced by the nonuniform separation during the cooling-down. It is also necessary to optimize the HCRE process conditions for improvement of the FS *m*-GaN quality.

Conclusions

In conclusion, a 200- μm -thick, crack- and stress-free 2-in.-diameter FS *m*-GaN wafer was successfully fabricated through a novel in-situ self-separation method with an *m*-sapphire substrate using HCRE in HVPE. At a high temperature of 1050 °C in a gas flow containing HCl, multiple voids were formed at the interface between *m*-sapphire and *m*-GaN by HCRE. The cross-sectional TEM showed that void formation mechanism was closely associated with preferential etching at HDRs such as SFs and TDs in the *m*-GaN layer. The self-separation of the thick GaN layer occurred during the cooling process because of thermal stress between *m*-sapphire and *m*-GaN. The Raman and PL measurements showed that the FS *m*-GaN wafer was almost stress-free. It is supposed that the proposed technique will allow a major breakthrough not only in the preparation of FS *m*-GaN substrates but also in the preparation of FS polar or semipolar GaN and AlN substrates by HVPE.

Acknowledgements

This work was supported by a grant from the Fundamental R&D Program for Technology of World Premier Materials (No. 10037904), funded by the Ministry of Trade, Industry and Energy, Republic of Korea. And the authors would like to thank M. K. Choi at the Raman Research Center for her scientific advice concerning about micro-Raman scattering analysis. And the authors also acknowledge D. W. Choi and D. J. Shin from Lumistal Co., Ltd. for the technical support.

Notes and references

- S. Nakamura, M. Senoh and T. Mukai, *Appl. Phys. Lett.*, 1993, **62**, 2390.
- P. Waltereit, O. Brandt, A. Trampert, H.T. Grahn, J. Meininger, M. Ramsteiner, M. Reiche and K.H. Ploog, *Nature (London)*, 2000, **406**, 865.
- B. Imer, F. Wu, M. D. Craven, J. S. Speck and S. P. Denbaars, *Jpn. J. Appl. Phys.*, 2006, **45**, 8644.
- M. McLaurin, T. E. Mates and J. S. Speck, *Appl. Phys. Lett.*, 2005, **86**, 262104-1.
- B. A. Haskell, A. Chakraborty, F. Wu, H. Sasano, P. T. Fini, S. P. Denbaas, J. S. Speck and S. Nakamura, *Journal of Electronic Materials*, 2005, **34**, 357.
- N. F. Gardner, J. C. Kim, J. J. Wierer, Y. C. Shen and M. R. Krames, *Appl. Phys. Lett.*, 2005, **86**, 111101.
- X. Ni, M. Wu, J. Lee, X. Li and A. A. Baski et al. *Appl. Phys. Lett.*, 2009, **95**, 111102.
- A. Kobayashi, S. Kawano, Y. Kawaguchi, J. Ohta and H. Fujioka, *Appl. Phys. Lett.*, 2007, **90**, 041908.
- R. Armitage and H. Hirayama, *Appl. Phys. Lett.*, 2008, **92**, 092121.
- H. Sasaki, H. Sunakawa, N. Sumi, K. Yamamoto and A. Usui, *J. Cryst. Growth*, 2009, **311**, 2910.
- T. Zhu, D. Martin and N. Grandjean, *Jpn. J. Appl. Phys.*, 2009, **48**, 020226.
- H. J. Lee, K. Fujii, T. Goto, T. Yao and Jiho Chang, *Appl. Phys. Lett.*, 2011, **98**, 071904.
- D. Hanser, L. Liu, E.A. Preble, K. Uduary, T. Paskova and K.R. Evans, *J. Cryst. Growth*, 2008, **310**, 3953.
- K. Fujito, K. Kiyomi, T. Mochizuki, H. Oota, H. Namita, S. Nagao and I. Fujimura *Phys. Stat. Sol. (a)*, 2008, **205**, 1056.
- H. M. Kim, J. E. Oh and T. W. Kang, *Mater. Lett.*, 2001, **47**, 276.
- M. K. Kelly, R. P. Vaudo, V. M. Phanse, L. Görgens, O. Ambacher and M. Stutzmann, *Jpn. J. Appl. Phys.*, 1999, **38**, L217.
- Y. Oshima, T. Eri, M. Shibata, H. Sunakawa, K. Kobayashi, T. Ichihashi and A. Usui, *J. Cryst. Growth*, 2004, **273**, 38.
- D. Gogova, A. Kasic, H. Larsson, C. Hemmingsson, B. Monemar, F. Tuomisto, K. Saarinen, L. Dobos, B. Pécz, P. Gibart and B. Beaumont, *J. Appl. Phys.*, 2004, **96**, 799.
- C. L. Chao, C. H. Chiu, Y. J. Lee, H. C. Kuo, P. C. Liu, J. D. Tsay and S. J. Cheng, *Appl. Phys. Lett.*, 2009, **95**, 051905.
- L. Zhang, Y. Shao, X. Hao, Y. Wu, H. Zhang, S. Qu, X. Chen and X. Xu, *CrystEngComm*, 2011, **13**, 5001.
- L. Zhang, Y. Dai, Y. Wu, Y. Shao, Y. Tian, Q. Huo, X. Hao, Y. Shen and Z. Hua, *CrystEngComm*, 2014, **16**, 9063
- H. Sasaki, H. Sunakawa, N. Sumi, K. Yamamoto, and A. Usui, *Phys. Status Solidi A*, 2009, **206**, 1160.
- S. H. Woo, M. H. Kim, B. C. So, G. H. Yoo, J. J. Jang, K. S. Lee, and O. H. Nam, *J. Cryst. Growth*, 2014, **407**, 6
- S. Y. Zhang, X. Q. Xiu, X. M. Hua, Z. L. Xie, B. Liu, P. Chen, P. Han, H. Lu, R. Zhang, and Y. D. Zheng, *Chin. Phys. B*, 2014, **23**, 058101
- J. H. Kim, C. S. Oh, Y. H. Ko, S. M. Ko, K. Y. Park, M. H. Jeong, J. Y. Lee, and Y. H. Cho, *Cryst. Growth Des.*, 2012, **12**, 1292
- T. B. Wei, J. K. Yang, Q. Hu, R. F. Duan, Z. Q. Huo, J. X. Wang, Y. P. Zeng, G. H. Wang, and J. M. Li, *J. Cryst. Growth.*, 2011 **314**, 141
- D. Du, D. J. Srolovitz, M. E. Coltrin and C. C. Mitchell *Phys. Rev. Lett.* 2005, **95**, 155503
- Q. Sun, C. D. Yerino, T. S. Ko, Y. S. Cho, I. H. Lee, J. Han and M. E. Coltrin *J. Appl. Phys.* 2008, **104**, 093523
- V. Jindal, and F. Shahedipour-Sandvik, *J. Appl. Phys.*, 2009, **106**, 83115.
- B. Leung, Q. Sun, C. D. Yerino, J. Han and M. E. Coltrin, *Semicond. Sci. Technol.*, 2012, **27**, 024005

PAPER

CrystEngComm

- 31 J. H. Choi and D. Y. Kim, *J. Am. Ceram. Soc.*, 1997, **80**, 62.
- 32 D. Tsivion, M. Schwartzman, R. Popovitz-Biro and E. Joselevich, *ACSnano*, 2012, **6**, 6433.
- 33 H. Gao, F. Yan, H. Zhang, J. Li, J. Wang and J. Yan, *J. Appl. Phys.*, 2007, **101**, 103533.
- 34 C. L. Chao, C. H. Chiu, Y. J. Lee, H. C. Kuo, P. C. Liu, J. D. Tsay and S. J. Cheng, *Appl. Phys. Lett.*, 2009, **95**, 051905
- 35 C. Kisielowski, J. Krüger, S. Ruvimov, T. Suski, J. W. Ager III, E. Jones, Z. Liliental-Weber, M. Rubin, E. R. Weber, M. D. Bremser and R. F. Davis, *Phys. Rev. B*, 1996, **54**, 17747.